

Investigation of Spatial Aliasing Artifacts of Wave Field Synthesis for the Reproduction of Moving Virtual Point Sources

Gergely Firtha, Peter Fiala

Budapest University of Technologies and Economics, Email: firtha,fiala@hit.bme.hu

Introduction

The aim of *sound field synthesis (SFS)* is the physical reproduction of an arbitrary sound field over an extended listening area applying a dense ensemble of loudspeakers –termed as the *secondary source distribution (SSD)*– driven with a properly chosen *driving function*. In the aspect of synthesizing dynamic sound fields the reproduction of moving virtual sources is of primary importance. The possibilities for the synthesis of moving sources have been investigated in several researches in the last decades [1, 2]. In recent articles driving functions were given by the present authors for the synthesis of uniformly moving virtual point sources in spatio-temporal, spatio-angular frequency and wave number-angular frequency domains, by utilizing traditional *Wave Field Synthesis (WFS)* [3] and the *Spectral Division Method (SDM)* [4] techniques. General WFS and SDM theories assume infinite linear continuous set of point sources as SSD. In practice the SSD is of finite extent, consisting of discrete source elements. The effect of spatial discretization –resulting in *spatial aliasing*– is well studied in the aspect of stationary virtual source models [5, 6], however –in the lack of an appropriate spectral description of the dynamic SFS problem– so far only qualitative investigation has been given for the spatial aliasing related to moving sources [7, 2]. In the present study a qualitative description of these artifacts is given relying on the semi-spectral and full-spectral SFS solutions.

Effects of SSD discretization

Consider a linear SSD at $\mathbf{x}_0 = [x_0, 0, 0]^T$, consisting of a continuous distribution of 3D point sources, weighted by the driving function $D(x_0, \omega)$. The synthesized field is given by the sum of the radiated field of individual SSD elements, reading

$$P(\mathbf{x}, \omega) = \int_{-\infty}^{\infty} D(x_0, \omega) G(\mathbf{x} - x_0, y, z, \omega) dx_0, \quad (1)$$

with $G(\mathbf{x}, \omega)$ being the 3D free-field Green's function describing the field of an acoustic point source. Performing a Fourier-transform along x_0 yields the synthesized field in the wavenumber domain:

$$\tilde{P}(k_x, y, 0, \omega) = \tilde{D}(k_x, \omega) \tilde{G}(k_x, y, 0, \omega), \quad (2)$$

with restricting the investigation to the $z = 0$ *synthesis plane*.

In practical applications the SSD is not continuous, but consists of equidistant sources. This discrete nature of

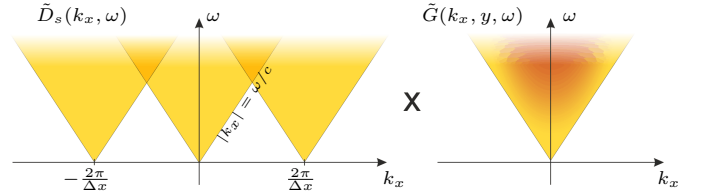


Figure 1: Calculation of the synthesized field in the wavenumber domain as the product of the sampled driving function and the Green's function spectra, given by $\tilde{G}(k_x, y, \omega) = -\frac{j}{4} H_0^2 (-j\sqrt{k_x^2 - k^2} |y|)$. Similarly to \tilde{G} , the energy of the ideal driving function is concentrated to $|k_x| < \frac{\omega}{c}$, termed the *propagation region*.

the SSD is modeled as the spatial sampling of the driving function with a sampling function [5]. As a well-known fact, the sampling of an arbitrary signal causes spectral repetition of the original spectrum at the multiples of the sampling frequency. The sampled driving function reads in the wavenumber domain as

$$\tilde{D}_s(k_x, \omega) = \sum_{\eta=-\infty}^{\infty} \tilde{D}\left(k_x - \eta \frac{2\pi}{\Delta x}, \omega\right), \quad (3)$$

with Δx being the sampling distance. Obviously, in the reproduced field overlapping spectral components will be present, causing audible distortion, termed as *spatial aliasing*. Refer to figure 1 for the illustration.

Moving source driving functions

For a virtual moving point source the driving functions can be derived either by using general WFS theory or the SDM. WFS stems from the stationary phase approximation of the Rayleigh-integral formulation of an arbitrary sound field, containing implicitly the driving functions [8]. Spectral Division Method –as an explicit solution– solves (2) for $\tilde{D}(k_x, \omega)$ with the target field and the Green's function written on a fixed $y = y_{\text{ref}}$ line, termed as the *reference line* [9]. Both traditional WFS and SDM ends up in correct synthesis along the reference line.

In the authors recent articles both WFS and SDM driving functions were given for a moving point source [4, 3] and it was shown, that –similarly to the stationary case– WFS constitutes a high-frequency/far-field approximation of the SDM solution. In the present treatise the explicit solution is used to investigate the sampling artifacts.

Consider a moving point source, traveling parallel to the SSD at a uniform velocity v , oscillating at a constant angular frequency ω_0 , located at $\mathbf{x}_s(t) = [vt, y_s, 0]^T$. The

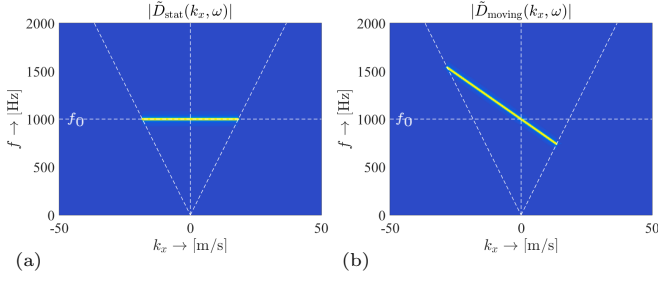


Figure 2: Comparison of the stationary (a) and moving source (b) driving function spectra. The moving source spectrum is obtained from the stationary spectrum by rotating around the source frequency ω_0 , with the rotation amount proportional to the source velocity and rescaled in order to fill the propagation region. The extrema of the moving source spectrum in ω are the perceived *dominant* frequencies of the virtual source approaching and diverging at $t \rightarrow \pm\infty$, given by $f_{a,d} = \frac{f_0}{1 \pm M}$, with $M = \frac{v}{c}$ being the Mach-number.

driving function to synthesize this moving source reads

$$\tilde{D}(k_x, \omega) = \frac{2\pi}{v} \frac{H_0^{(2)} \left(-j\sqrt{\left(\frac{\omega - \omega_0}{v}\right)^2 - k^2 |y_{\text{ref}} - y_s|} \right) \delta \left(k_x - \frac{\omega - \omega_0}{v} \right)}{H_0^{(2)} \left(-j\sqrt{k_x^2 - k^2 |y_{\text{ref}}|} \right)} \quad (4)$$

For a detailed derivation refer to [4]. The driving function contains the wavenumber content of a moving point source in its numerator, and that of the stationary Green's function in the denominator. One can note, that the wavenumber content of a moving source is a Dirac-distribution in k_x , reflecting the fact, that along the x -axis at arbitrary y position the measured time history –and the frequency content– of a source pass-by is space-invariant, only a phase shift is present. For an illustration of the driving functions for stationary and moving sources oscillating at $f_0 = 1$ kHz see figure 2.

Description of aliasing components

The spatial discretization model, described above can be applied to the moving source case directly: the spectral representation of the sampled driving function is obtained by substituting (4) into (3)

$$\tilde{D}_s(k_x, \omega) = \frac{2\pi}{v} H_0^{(2)} \left(-j\sqrt{\left(\frac{\omega - \omega_0}{v}\right)^2 - k^2 |y_{\text{ref}} - y_s|} \right) \sum_{\eta=-\infty}^{\infty} \frac{\delta \left(k_x - \eta \frac{2\pi}{\Delta x} - \frac{\omega - \omega_0}{v} \right)}{H_0^{(2)} \left(-j\sqrt{\left(k_x - \eta \frac{2\pi}{\Delta x}\right)^2 - k^2 |y_{\text{ref}}|} \right)} \quad (5)$$

and the synthesized field is given by (2)

$$\tilde{P}(k_x, y, 0, \omega) = -\frac{j}{4} \tilde{D}_s(k_x, \omega) H_0^{(2)} \left(-j\sqrt{k_x^2 - k^2 |y|} \right). \quad (6)$$

The aliased synthesized field is also described by series of Dirac-distributions, for which the inverse Fourier-transform can be performed analytically. After proper rearrangement the spatial inverse Fourier-transform of the synthesized field reads

$$P(x, y, \omega) = D(x, \omega) \sum_{\eta=-\infty}^{\infty} -\frac{j}{4} H_0^{(2)} \left(-j\sqrt{\left(\frac{\omega - \omega_0}{v} + \eta \frac{2\pi}{\Delta x}\right)^2 - \left(\frac{\omega}{c}\right)^2 |y|} \right) e^{-j\eta \frac{2\pi}{\Delta x} x}. \quad (7)$$

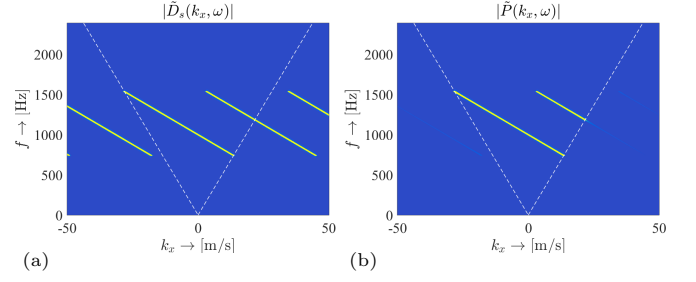


Figure 3: Spectra of the sampled driving function (a) and the synthesized field (b). High-frequency components –present in front of the moving source, where the local wavenumber is increased due to the Doppler-effect– are most likely to alias into the propagation region.

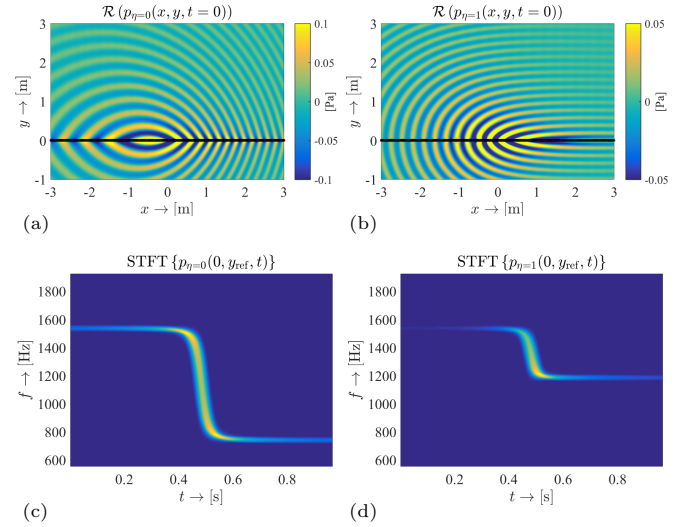


Figure 4: Spatial distribution of the ideal synthesized field, $\eta = 0$ (a) and the 1st aliasing component $\eta = 1$ (b) at the time origin, and the corresponding spectrogram, measured at $[0, y_{\text{ref}}, 0]^T$ (c-d). The virtual source travels parallel to the SSD with $\mathbf{x}_0(0) = [0, -1, 0]^T$ with $v = 150$ m/s, $\omega_0 = 2\pi \cdot 1000$ rad/s. The reference line was set to $y_{\text{ref}} = 1$ m. The SSD was discretized with a sampling distance $\Delta x = 0.2$ m.

Obviously, $\eta = 0$ gives the ideal, non-aliased synthesized field, while other η parameters describe the individual aliasing components. See figure 3 for an illustration. It is important to note, that unlike the stationary case, where the synthesized field is obtained in the form of a convolution (see Eq. (1)), here the synthesized field at $[x, y, 0]^T$ is yielded from the driving function at x by multiplying it with a transfer function. This transfer function describes the frequency content of moving sources measured at $[0, y, 0]^T$, traveling at the velocity v , oscillating at an altered source frequency $\omega'_0 = \omega_0 + \eta \frac{2\pi v}{\Delta x}$ (compare with [4, Eq. (11)])

This description allows us to investigate the aliasing components individually both regarding their spatial distribution and time evolution. As an example the ideal synthesized field and the first aliasing component are shown in figure 4. With the chosen simulation parameters only the presented aliasing component ($\eta = 1$) contributes considerably to the radiated field. The simulation reveals, that in front of the virtual source, (or in central position at $t < 0$) aliasing components propagate in dif-

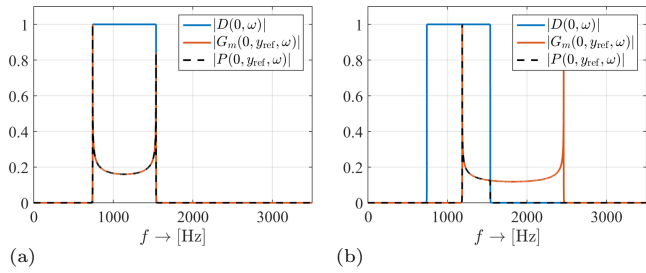


Figure 5: Description of the individual aliasing components as the intersection of the ideal driving function and the moving source Green’s function for $\eta = 0$ (a) and $\eta = 1$ (b).

ferent direction than the ideal field, but at the same perceived frequency. On the other hand behind the virtual source also the perceived frequency is altered. The direction of the spatial aliasing waves may be characterized by investigating the k_x values of the aliased spectra in figure 3(b), however in the followings we mainly deal with the time evolution of the synthesized field at fixed observation positions. The observations above show that in the total field

- the interference pattern of the aliasing components changes rapidly over the time. At a fixed listener position this causes audible variation in the time history of the total field amplitude, termed as *amplitude ringing*.
- various simultaneous frequency components will be present, termed here as *frequency ringing*. These undesired frequency components have been reported in the related literature [7, 2].

The latter frequency error can be observed in the spectrogram of the measured time histories, presenting an altered dominant frequency of the diverging in the aliasing components. Terminology „frequency ringing” refers to the interpretation of the undesired frequency component at $t \gg 0$ is caused by the pole of the SSDs Green’s function $\tilde{G}(k_x, y, \omega)$ at $|k_x| = \frac{\omega}{c}$, which leads to an emphasized aliasing components at these wavenumbers in the form of lateral waves (refer to figure 3 (b)).

Investigation of undesired frequency components

In order to characterize the ringing frequencies of the aliasing components, one should investigate the mathematical description aliasing components individually: As shown in Figure 5 the frequency content of the synthesized field at an arbitrary position is characterized by the intersection of the spectrum of the original driving function –bandlimited between the original dominant frequencies $\frac{\omega_0}{1 \pm M}$ – and the spectrum of a moving source, oscillating at an altered source frequency ω'_0 , defined in the previous section:

$$P_\eta(x, y, \omega, \omega_0) = D(x, \omega) G_{\text{mov}}(0, y, \omega, \omega_0 + \eta \frac{2\pi v}{\Delta x}) e^{-j\eta \frac{2\pi}{\Delta x} x}. \quad (8)$$

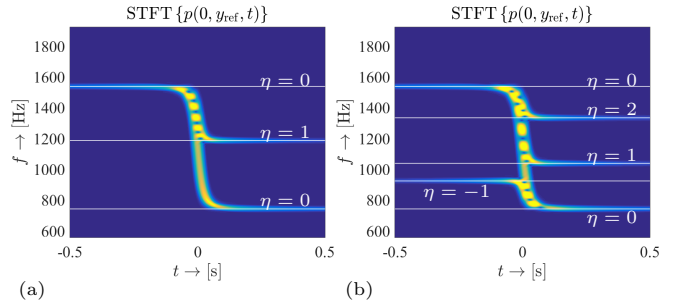


Figure 6: Spectrogram of the synthesized field at $[0, y_{\text{ref}}, 0]^T$, with the analytical ringing frequencies denoted by solid white line. The simulation parameters were $v = 150$ m/s, $\omega_0 = 2\pi \cdot 1000$ rad/s, $y_{\text{ref}} = 1$ m with $\Delta x = 0.2$ m for (a) and $\Delta x = 0.3$ m for (b)

The altered, lateral directed frequency ringing artifact stems from the lower pole of the moving source Green’s function, describing the altered dominant frequency perceived during the diverging. Having found the altered frequency ω'_0 the dominant frequencies, that will characterize the undesired frequency components are given as

$$\omega_{\text{ringing}} = \frac{1}{1 \pm M} \left(\omega_0 + \eta \frac{2\pi v}{\Delta x} \right). \quad (9)$$

Obviously, for aliasing components with $\eta > 0$ the lower dominant frequency, for components with $\eta < 0$ the higher dominant frequency will cause frequency ringing after and before the virtual source pass-by respectively.

The validity of this frequency localization is verified by comparing the measured and analytical ringing frequencies, presented in Figure 6. In Figure 6 (b) the sampling distance is increased, so that higher order aliasing artifacts are present in the synthesis: $\eta = 1, 2$ from the upper sideband and $\eta = -1$ from the lower sideband, i.e. even the dominant frequency of the diverging is higher, than the corresponding angular frequency for the half of the sampling wavenumber. The envelope of the spectrograms also present the amplitude ringing, mentioned above.

Reducing spatial aliasing artifacts

Traditional techniques attempt to avoid spatial aliasing by simple anti-aliasing filtering of the driving functions. As a simple solution one may bandlimit the driving function to $|k_x| < \frac{\pi}{\Delta x}$, therefore no overlapping components may remain in the synthesized field. However if this approach is applied for the moving source case the following problem holds: by investigating figure 3 with simple geometrical considerations it becomes clear, that bandlimiting the driving function in k_x is equivalent to low-pass filtering in ω to a cut-off frequency $\omega_c = \omega_0 + \frac{v\pi}{\Delta x}$. Besides this, the poles in the aliasing components remain unchanged in the synthesized field, therefore the undesired frequency ringing still occurs. Traditional anti-aliasing therefore would end up in truncating the virtual source pass-by in the time domain with the spatial aliasing artifacts still present in the time history.

As a possible solution one should make use of the fact, that frequency ringing artifacts are lateral waves, emerg-

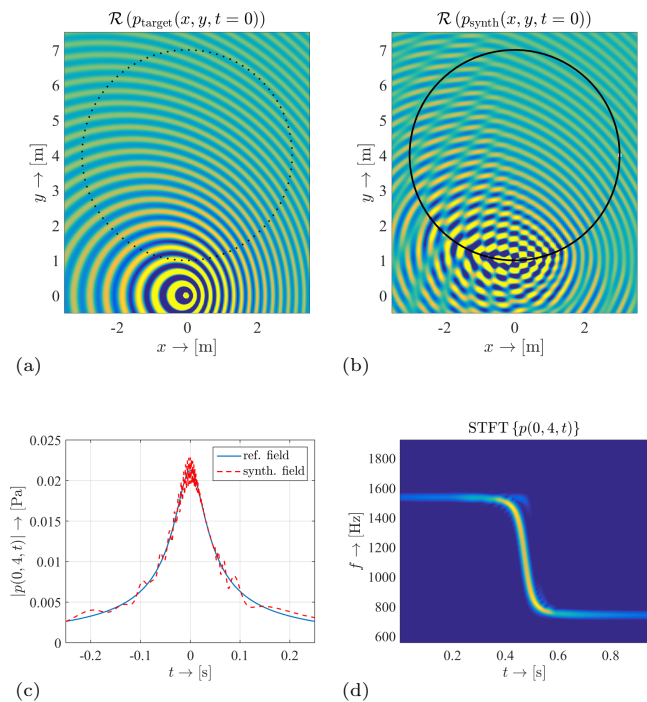


Figure 7: Spatial distribution of the target sound field (a) and the synthesized field (b) with the amplitude (c) and the spectrogram (d) of the measured time history for the case of a circular SSD. The simulation parameters were $v = 120$ m/s, $\omega_0 = 2\pi \cdot 1000$ rad/s, $\Delta x = 0.2$ m

ing from SSD elements located at $|x| \gg 0$ (i.e. far from the central position). If one eliminates these SSD elements by choosing a non-linear, enclosing SSD the frequency ringing artifacts may be suppressed. This intuitive solution can be formulated mathematically as suppressing the poles of the Green's function, by choosing a problem geometry, in which the spectral decomposition coefficients of the Green's function does not exhibit poles.

One feasible choice may be the use of a circular secondary source array. For such an ensemble the moving source WFS driving functions were used, presented in [3], with referencing the synthesis to the center of the SSD. The result of synthesis is shown in figure 7. The spatial distribution of the synthesized field 7(b) suggests, that aliasing components are present in the synthesized field, causing amplitude ringing in the measured time history due to the temporally varying interference. These effects can be observed on the amplitude of the measured time history 7(c): obviously as long as any spatial aliasing component is present in the synthesis (which holds for every practical case) these amplitude ringing effects can not be avoided. Figure 7(d) however suggests, that the frequency ringing artifacts can be avoided based on the foregoing.

Conclusion

In the present treatise a quantitative analysis was given on the spatial aliasing artifact present in the synthesis of a moving virtual point sound source. A mathematical formulation was derived for the description of the individual aliasing component both in the wavenumber-frequency and in the spatio-frequency domain. It was

shown, that in case of a linear SSD two main components are present in the synthesized field: amplitude ringing, due to the time varying interference pattern of the aliasing components and the ideal field, and a frequency ringing, due to the fact, that aliasing waves with different perceived frequencies propagate in different directions than the corresponding waves in the ideal field. The first is present at the synthesized field as a variation in the amplitude of the time history, measured at an arbitrary position and can not be eliminated as long as any aliasing component is present in the synthesized field. The latter causes undesired frequency coloration most likely during the diverging of the virtual source. Traditional anti-aliasing strategies result in serious artifacts when applied for a moving virtual source, since they result in simple low-pass filtering with respect to the angular frequency, but leaving the frequency coloration effects unchanged. It was proved through simulations, that enclosing secondary source arrays may suppress the frequency ringing effects almost completely, as it was demonstrated via the example of the synthesis with a circular SSD.

References

- [1] J. Ahrens and S. Spors. Reproduction of Moving Virtual Sound Sources with Special Attention to the Doppler Effect. In *Proc. of the 124th Audio Eng. Soc. Convention*, Amsterdam, May 2008.
- [2] J. Ahrens. *Analytic Methods of Sound Field Synthesis*. Springer, Berlin, 1st edition, 2012.
- [3] G. Firtha and P. Fiala. Wave Field Synthesis of Moving Sources with Retarded Stationary Phase Approximation. *J. Audio Eng. Soc.*, 63(12):958–965, Dec. 2015.
- [4] G. Firtha and P. Fiala. Sound Field Synthesis of Uniformly Moving Virtual Monopoles. *J. Audio Eng. Soc.*, 63(1/2):46–53, Jan./Feb. 2015.
- [5] S. Spors. Investigation of spatial aliasing artifacts of wave field synthesis in the temporal domain. In *in 34rd German Annual Conference on Acoustics (DAGA)*, Dresden, March 2008.
- [6] S. Spors and J. Ahrens. Spatial sampling artifacts of wave field synthesis for the reproduction of virtual point sources. In *Proc. of the 126th Audio Eng. Soc. Convention*, Munich, May.
- [7] A. Franck, A. Graefe, K. Thomas, and M. Strauss. Reproduction of Moving Sound Sources by Wave Field Synthesis: An Analysis of Artifacts. In *Proc. of the 32nd Intl. Conf. Audio Eng. Soc.: DSP For Loudspeakers*, Hillerød, Sept. 2007.
- [8] E.N.C. Verheijen. *Sound Reproduction by Wave Field Synthesis*. PhD thesis, Delft University of Technology, 1997.
- [9] J. Ahrens and S. Spors. Sound Field Reproduction Using Planar and Linear Arrays of Loudspeakers. *IEEE Trans. Audio, Speech, Lang. Process.*, 18(8):2038–2050, Nov. 2010.